EVLA Memo 134
EVLA Polarizer Stability at C and K Bands

Rick Perley and Bob Sault

June 3, 2009

Abstract

Requirements for the cross-polarization stability necessary to enable noise-limited polarimetric imaging are derived. Observations to determine the EVLA's polarimetric stability were taken at C-band and K-band. The stability in the 'D' terms over ∼8 hours is typically better than 0.1% at C-band, and 0.2% at K-band. The cross-polarization remains constant to better than ∼ 0.2% over a duration of ∼ 2 weeks for most antennas at C-band. This level of stability is sufficient for noise-limited polarimetry in all but the most demanding cases where > 1 Jy in total intensity is in the field. For these, it is shown that a version of polarization self-calibration will remove time-variable cross-polarization.

1 Introduction

The EVLA has set a goal of noise-limited imaging in all Stokes parameters over the full primary beam for observations of arbitrary duration. Meeting this goal will require highly stable polarizers, software to permit accurate measurement of and correction for the cross-polarization, plus software to remove the spatially variant polarization due to the antenna optics.

In this memo, we set out the essential stability requirements for attaining the EVLA's polarimetry goals, demonstrate the current level and stability of two of the EVLA's polarizer designs, and show that for the most demanding polarimetry, polarization self-calibration should enable noise-limited imaging for those cases where the strong source is on-axis. The issue of correcting for antenna beam polarization is not addressed in this memo.

2 Generalized Interferometer Response

The most general form for the response of a complex correlator to arbitrarily polarized radiation was derived by Morris, Radhakrishnan and Seielstad in 1964, and can be written in a compact matrix form as:

$$\mathbf{V} = \mathbf{GPRS} \tag{1}$$

where $\mathbf{V}$ is the interferometer response vector, $\mathbf{S}$ is the Stokes visibility vector, and $\mathbf{G}$, $\mathbf{P}$, and $\mathbf{R}$ are 4 x 4 matrices describing the antenna gains, cross-polarization, and orientation with respect to the sky, respectively[1]. All quantities are complex and are defined as (in a circular basis):

$$\mathbf{V} = \begin{pmatrix} V_{r1r2} \\ V_{l1l2} \\ V_{r1l2} \\ V_{l1r2} \end{pmatrix} \mathbf{G} = \begin{pmatrix} G_{r1}G^*_{r2} & 0 & 0 & 0 \\ 0 & G_{l1}G^*_{l2} & 0 & 0 \\ 0 & 0 & G_{r1}G^*_{l2} & 0 \\ 0 & 0 & 0 & G_{l1}G^*_{r2} \end{pmatrix} \mathbf{P} = \begin{pmatrix} 1 & D_{r1}D^*_{r2} & D^*_{r2} & D_{r1} \\ D_{l1}D^*_{l2} & 1 & D_{l1} & D^*_{l2} \\ D^*_{l2} & D_{r1} & 1 & D_{r1}D^*_{l2} \\ D_{l1} & D^*_{r2} & D_{l1}D^*_{r2} & 1 \end{pmatrix}$$

$$\mathbf{R} = \begin{pmatrix} e^{-i\Delta\Psi_p} & 0 & 0 & 0 \\ 0 & e^{i\Delta\Psi_p} & 0 & 0 \\ 0 & 0 & e^{-i\Sigma\Psi_p} & 0 \\ 0 & 0 & 0 & e^{i\Sigma\Psi_p} \end{pmatrix} \mathbf{S} = \begin{pmatrix} I+V \\ I-V \\ Q+iU \\ Q-iU \end{pmatrix}$$

[1]Strictly speaking, each of the four Stokes vector components of $\mathbf{S}$ should be divided by two. Unfortunately, all popular interferometry calibration/imaging packages utilize the definitions shown. The omission is made up in the inversion to visibilities.

In these expressions, V_{mn} are the raw complex visibilities as measured by the correlator, the G_m represent the complex instrumental gains, and I, Q, U, and V are the complex Stokes visibilities. The elements in the rotation matrix are defined as $\Delta\Psi_p = \Psi_{p1} - \Psi_{p2}$ and $\Sigma\Psi_p = \Psi_{p1} + \Psi_{p2}$, where Ψ_{pi} is the parallactic angle of antenna i. The elements in the polarization matrix are defined as:

$$D_r = \tan\beta_r e^{2i\phi_r} \quad (2)$$
$$D_l = \tan\beta_l e^{-2i\phi_l}. \quad (3)$$

The angles ϕ_r and ϕ_l physically represent the orientation of the major axis of the polarization ellipse for the REP and LEP ports, respectively. The angle β is defined as

$$\beta_r = \pi/4 + \chi_r \quad (4)$$
$$\beta_l = \pi/4 - \chi_l \quad (5)$$

and physically represents the deviation of the antenna polarization ellipticity from perfect circularity. The angle $\chi = \arctan(b/a)$ is the ellipticity of the antenna polarization ellipse in the antenna frame of reference[2]. Left elliptical polarization has positive ellipticity, right elliptical polarization is negative. The assumption of low antenna cross-polarization means that $\beta \ll 1$. As defined above, both β_r and β_l are positive real quantities. There are no approximations employed in this formulation, which despite being written in a circular basis can be employed for a linear polarization basis as well.

In principle, if the gains, cross-polarizations, and antenna parallactic angles are all known, Equation (1) can be inverted to provide the desired Stokes visibilities. Limitations in the fidelity of the imaging will be generated by (amongst many other things), errors or variability in any of these calibration characteristics.

3 Approximations Appropriate for This Study

We are interested in deriving a simple expression showing how variations in antenna cross-polarization will limit polarimetric imaging. The analysis is considerably simplified if we make some approximations:

- Stokes parameters V and U are both zero. The former is justified as $V/I << 1$ for the great majority of calibrator sources. The latter assumption simply assumes a rotation of the reference frame to align with the source's plane of polarization, which in no way limits the generality of our analysis.
- Both the antenna cross-polarization D and the fractional linear polarization Q/I are much less than one, so that 2nd order products can be ignored. Both are well justified for well-designed polarizers and most sources.
- All $G = 1$. All data are presumed well calibrated for parallel-hand gain variations.
- The Stokes visibilities I and Q are real, with no dependence on baseline length or orientation. In practice, this means we are considering a point source at the phase center. There is no loss in generality with this.
- The parallactic angle $\Psi_p = 0$ for all antennas. This is done for convenience.

None of these simplifications will sigificantly affect the conclusions derived from the following analysis.

With these assumptions, the relationships between the observed complex visibilties V_{mn} and the Stokes visibilities Q and I can be written:

$$V_{r_1r_2} = I \quad (6)$$
$$V_{l_1l_2} = I \quad (7)$$
$$V_{r_1l_2} = [(D_{r1} + D^*_{l2})I + Q] \quad (8)$$
$$V_{l_1r_2} = [(D_{l1} + D^*_{r2})I + Q] \quad (9)$$

The presence of the terms in I in the cross-hand responses represents the effects of an imperfect polarizer – these are termed 'leakages' as they describe how total intensity 'leaks' into the correlations which contain the linear polarization information. We note that there are two ways to eliminate these unwanted contributions:

[2]Thus, a CW signal applied to each of the two polarized ports of the antenna will generate, in the far field, an elliptically polarized response characterized by a position angle ψ with ellipticity χ. An incoming wave of that orientation and ellipticity is perfectly matched to that port.

1. Have perfect polarizers, for which $\beta = 0$, and thus $D = 0$.
2. For imperfect polarizers, arrange that the REP and LEP polarization ellipses of the two antennas for each baseline are orthogonal ($\phi_r = \phi_l \pm \pi/2$) and have equal ellipticity ($\beta_r = \beta_l$), in which case the two 'D' terms are equal and opposite. This is known as the 'orthogonality condition'[3].

Unfortunately, neither condition can be met in practice with suitable accuracy to enable the desired precision in polarimetric imaging, although absolute measurements of the 'D'-terms at C-band by Perley (EVLA Memo #133) show that orthogonality is sufficient to considerably reduce the apparent cross-polarization on each baseline.

4 Estimating the Effects of Polarization Leakage

We consider the image response at the phase center. Because the sky brightnesses in all Stokes are real, each visibility is added to its complex conjugate, so that at the phase center, the observed image responses for Stokes I and Q are, for each baseline:

$$I_{obs} = (V_{r1r2} + V_{l1l2} + V^*_{r1r2} + V^*_{l1l2})/4 \quad (10)$$

$$Q_{obs} = (V_{r1l2} + V_{l1r2} + V^*_{r1l2} + V^*_{l1r2})/4 \quad (11)$$

It is straighforward to show that, for N_a antennas, these observed responses are related to the true values I and Q (to the level of our approximations) by

$$I_{obs} = I \quad (12)$$

$$Q_{obs} = Q + \frac{I}{N_a}\sum_{i=1}^{N_a}(\beta_{ri}\cos 2\phi_{ri} + \beta_{li}\cos 2\phi_{li}) \quad (13)$$

Note that only the variations in the real part of the 'D' terms affect the response in 'Q' at the phase center.

The effects of the polarization leakages are correctable so long as the 'D' terms remain constant for a time sufficient to permit their estimation to the necesssary accuracy. For the VLA, the solution interval is normally a few hours in order that there be a sufficient change in antenna parallactic angle to permit a separation of the antenna and source polarizations. In reality, the amplitude and/or phase of the cross-polarization terms will change over time. The effect of a changing cross-polarization can be estimated with the following simple argument.

Assume that the real parts of the complex leakages $\beta\cos(2\phi)$ for each of the $2N_a$ contributing terms in Eqn. 13 are varying independently with an amplitude $\delta\beta$ over some time scale t. For any one time (*i.e.*, a snapshot observation), the variation in the observed value of Q_{obs} from the correct value Q, for N_a antennas, can be shown to be

$$\delta Q \sim \sqrt{\frac{2}{N_a}} I\delta\beta \quad (14)$$

If $N_t = T/t$ is the number of time intervals over total time T, each of which has values of β randomly different by typical size $\delta\beta$ from the mean, then the typical error in the determined value of Q_{obs} becomes

$$\delta Q \sim \sqrt{\frac{2}{N_a N_t}} I\delta\beta \quad (15)$$

5 Application One – Polarization of a Strong Source

Now consider a strong, isolated source, and ask 'what is the accuracy of the determination of the fractional polarization'. Defining the fractional polarization $P = Q/I$, the error δP due to variations in the leakage is then

$$\delta P \sim \sqrt{\frac{2}{N_a N_t}} \delta\beta. \quad (16)$$

[3]Note that meeting this condition only prevents Stokes 'I' from entering the cross-hand correlations. It will not prevent Stokes 'V' from contaminating these correlations, nor prevent Stokes 'Q' or 'U' from contaminating the parallel hand correlations.

For the VLA, $N_a = 27$. Determining the number of 'independent observations' is more subjective. For the sake of argument, assume the variations are randomized on an hourly timescale, and take $N_t = 8$. Then,

$$\delta P \sim \delta\beta/10. \tag{17}$$

The error in the determination of the fractional polarization is typically lower than the variation in the antenna polarization by an order of magnitude. If we set the requirements for the accuracy to be 0.1% (*i.e.* $\delta P = 10^{-3}$), then the requirement for the stability in the antenna polarization is only ∼1%. We show in this memo that this stability is easily met by the EVLA polarizers.

6 Application Two– Noise Limited Polarimetry in the Presence of a Dominant Source

Consider an observation of a weak source located adjacent to a very strong point source. Following the argument above, the accuracy of the determination of the polarization for the strong source is about 10% of the stability of the antenna cross-polarization. The scattered I intensity signal which appears in the Q image is however not confined to the location of the strong source as it is coupled to the Q image with an essentially random phase which originates within the polarizer. Because of this phase scattering, the coupled 'I' signal will appear approximately uniformly all over the image, so that the estimation of the error in Stokes Q at the phase center will serve as an estimation of the scattered noise in all other cells of the image.

In order to measure the weak source's polarized signal, the cross-polarized scattered flux from the nearby strong source must be much less than true polarized signal from the target. In the worst case, the scattered 'I' intensity appearing in the 'Q' image must be less than the thermal noise, σ. From equation 15 we can then set the limit

$$\delta\beta < \frac{\sigma}{I}\sqrt{\frac{N_a N_t}{2}} \tag{18}$$

which for our 'typical' example, gives

$$\delta\beta < \frac{10\sigma}{I} \tag{19}$$

The ratio σ/I can be very small for the EVLA – of order 10^{-7} in the most extreme cases (1μJy noise for a 10 Jy object). Our simple analysis indicates that to achieve noise-limited polarimetry, polarizer stability on the order of 1 part in a million will be required! Observations indicate a stability, at best, of one part in 10^4, which indicates noise-limited polarimetry will be achieved in deep integrations for fields containing no more than about 200 mJy in background objects, in the absence of a means of tracking and correcting for small changes in antenna cross-polarization. This level should be sufficient for most fields – the 'typical' background source in a random L-band observation is about 100 mJy.

For fields containing more powerful objects, the small changes in antenna cross-polarization must be tracked and corrected for via a sort of polarization self-calibration. We discuss this later in this memo.

7 Observations

The primary goal of these observations was to determine the magnitude and stability of the cross-polarization for the EVLA's polarizers. The EVLA employs three different polarizer designs. We consider here two of these. For three of the high frequency bands (Ku, K, Ka) a waveguide polarizer is utilized. It is currently deployed at K-band on all (both EVLA and VLA) antennas. At the low frequency bands (L, S, and C) the waveguide design is both too large and of insufficient bandwidth, so an orthomode transducer (OMT) plus a wideband microwave quadrature hybrid is employed. This new OMT design is now being retrofitted into the C-band receivers – currently, eight EVLA antennas are equipped with these wideband systems. Our tests were conducted at K and C bands.

Accurate polarimetric observations are much simpler if the target source is both strong and unresolved. For the K-band observations we utilized 3C84, whose emission is dominated by a ∼15-Jy point source. With the array in the B-configuration, the weak extended halo emission associated with 3C84 is completely resolved out. For the C-band observations, both 3C84 and 0217+738 (a pure point source of about 4 Jy) were employed.

Although the shorter spacings saw the effects of the 3C84 halo at C-band, these were weak, and did not affect the results presented below in any notable way.

The observations were made in two sessions, all in continuum mode with 50 MHz bandwidth:

- Observations of 0217+738 at eight C-band frequencies over eight hours on the evening of 12 April 2009. The frequencies selected were 4385, 4885, 5385, 5885, 6385, 6885, 7385 and 7885 MHz. An observation of 3C48 at the beginning of the run was taken to establish the correct position angle.
- Observations of 0319+415 (3C84) at eight C-band frequencies and eight K-band frequencies over 9.5 hours on 26 April 2009. The C-band frequencies were the same as for the earlier observation. The K-band frequencies were 18265, 19265, 20515, 21515, 22765, 23765, 25015 and 26015 MHz. Single observations of 3C48 and 3C286 were taken at the beginning and end to establish the correct position angle.

The data were loaded to disk and edited via normal procedures. Closure errors, averaged over the duration of the observation, (mostly arising from the differing bandpasses between VLA and EVLA systems) were removed. Residual (time-variable) closure errors were measureable, and ultimately limited the dynamic range of Stokes I images. All the polarimetric analysis reported below was through the Miriad software package.

8 Results

8.1 Cross-Polarization Magnitude

Calibration shows the cross-polarization magnitude is typically 5 to 10% for the new C-band wideband polarizers, as reported in EVLA Memo #131. At K-band, the polarizations are much smaller, typically 2 – 5%.

8.2 Short-Term Stability

The critical question is the stability of the polarization over intervals of a few hours. For the most exacting polarimetry, it is probable that polarization calibration will be conducted at the same time as the observations, likely requiring long continuous observational blocks and carefully constructed calibration protocols. Figure 1 shows the polarization stability at eight frequencies for EVLA antenna 2, selected as typical for the better behaved antennas. This figure shows the variation in the real and imaginary parts of the cross-polarization leakage ('D') about the mean value determined from the entire duration. At all frequencies the peak deviation is less than 0.2%, and for most frequencies, the median deviation is about 0.05%. Some frequencies appear to be considerably more stable than others – no obvious explanation is offered.

Antenna 2 was typical for most of the EVLA antennas at that band. The most unstable antenna, – #15 – is shown in Fig. 2. For this antenna (which was the worst of the 8 antennas investigated), peak instability is about 0.3%, with a median of about 0.1%.

The K-band polarizers appear to be considerably less stable. We show the results from two antennas in Figures 3 – showing a typical antenna, and 4, which shows the most unstable antenna. In principle, time-varying pointing errors, combined with the off-axis polarimetric beam response, could contribute to the observed apparent instability. The target source for the K-band observing – 3C84 – transits near the zenith where pointing stability is known to be poorer than at the lower elevations where the other target source – 0217+738 – was observed. This possible explanation was investigated by reviewing the log of antenna reference pointing solutions. Although some correlation was found between the polarimetric stability and referenced pointing solutions, the observed cross-polarization variation is factors of a few larger than the effect predicted from the pointing offsets. We conclude that pointing errors are unlikely to be responsible for the variations in cross-polarization seen in the data.

8.3 Long-Term Stability

In the future, it is likely that observational programs which do not require the utmost in polarization fidelity will be scheduled in blocks, perhaps as short as 1 hour, potentially distributed over many days. In this observing scenario, dedicated polarization calibration cannot be done, and we will need to rely on separately determined antenna polarizations, likely determined in advance by days to weeks. This will be easily done provided the antenna polarizations are stable over long periods of time – hopefully as long as many weeks.

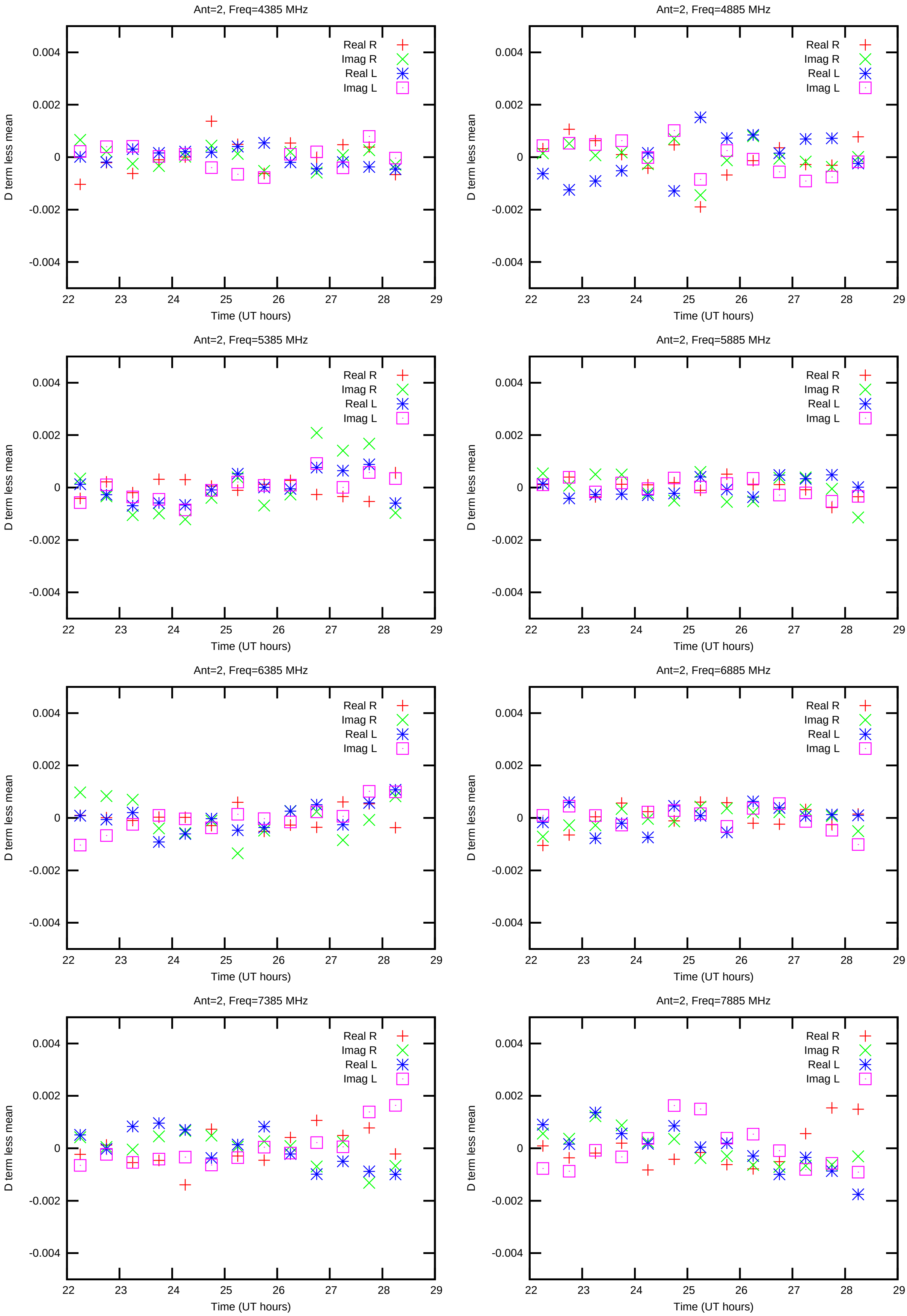

Figure 1: Polarization stability of antenna 2 at eight frequencies within C-band. Each panel shows the half-hour variation of the real and imaginary parts of the cross-polarization about the average value for both RCP and LCP. This antenna is typical of the majority, and shows the stability to be generally better than 0.1%.

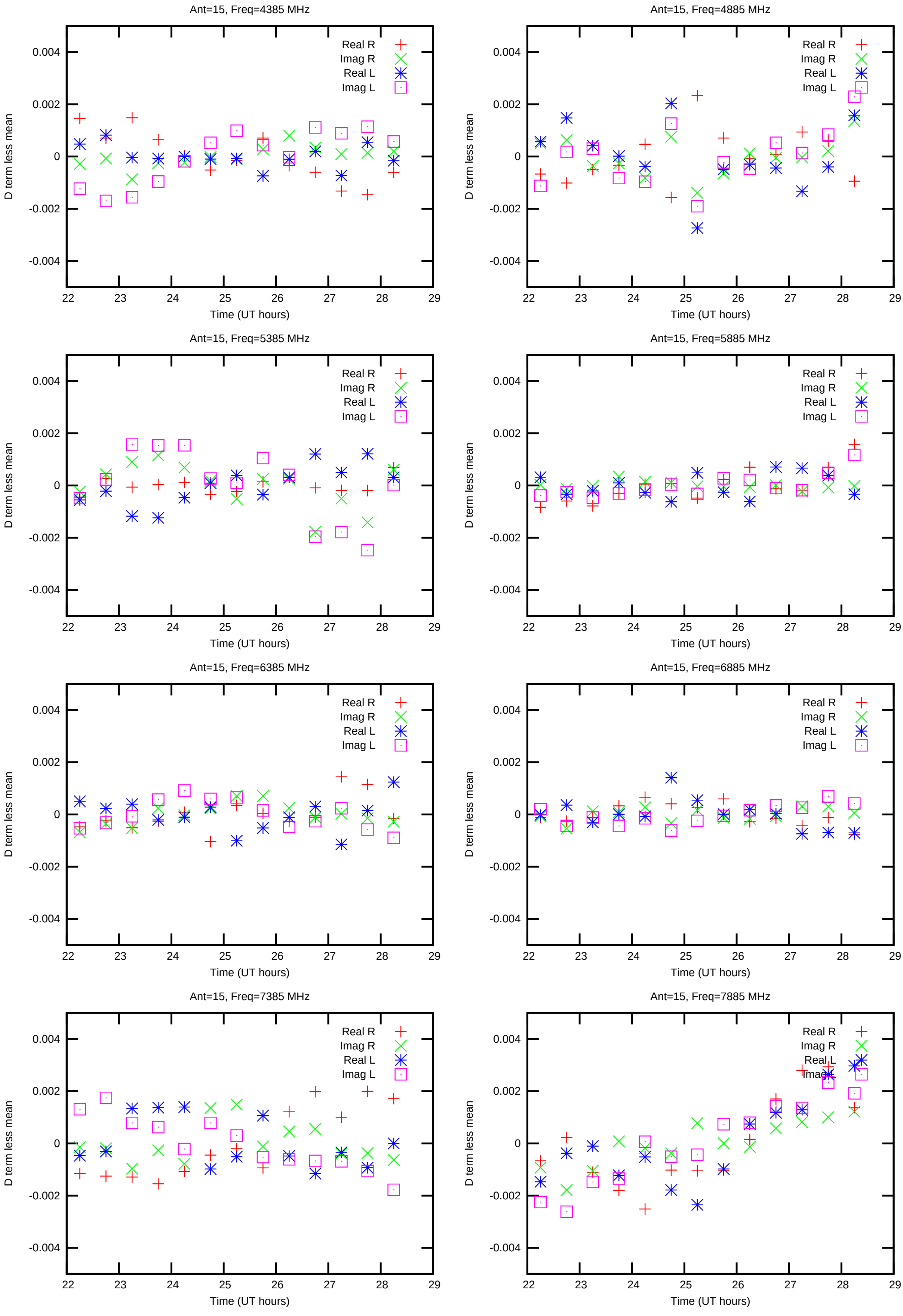

Figure 2: Polarization stability of antenna 15 at C-band. This antenna was the most unstable of the eight antennas equipped with the new wide-band polarizers at the time of this test.

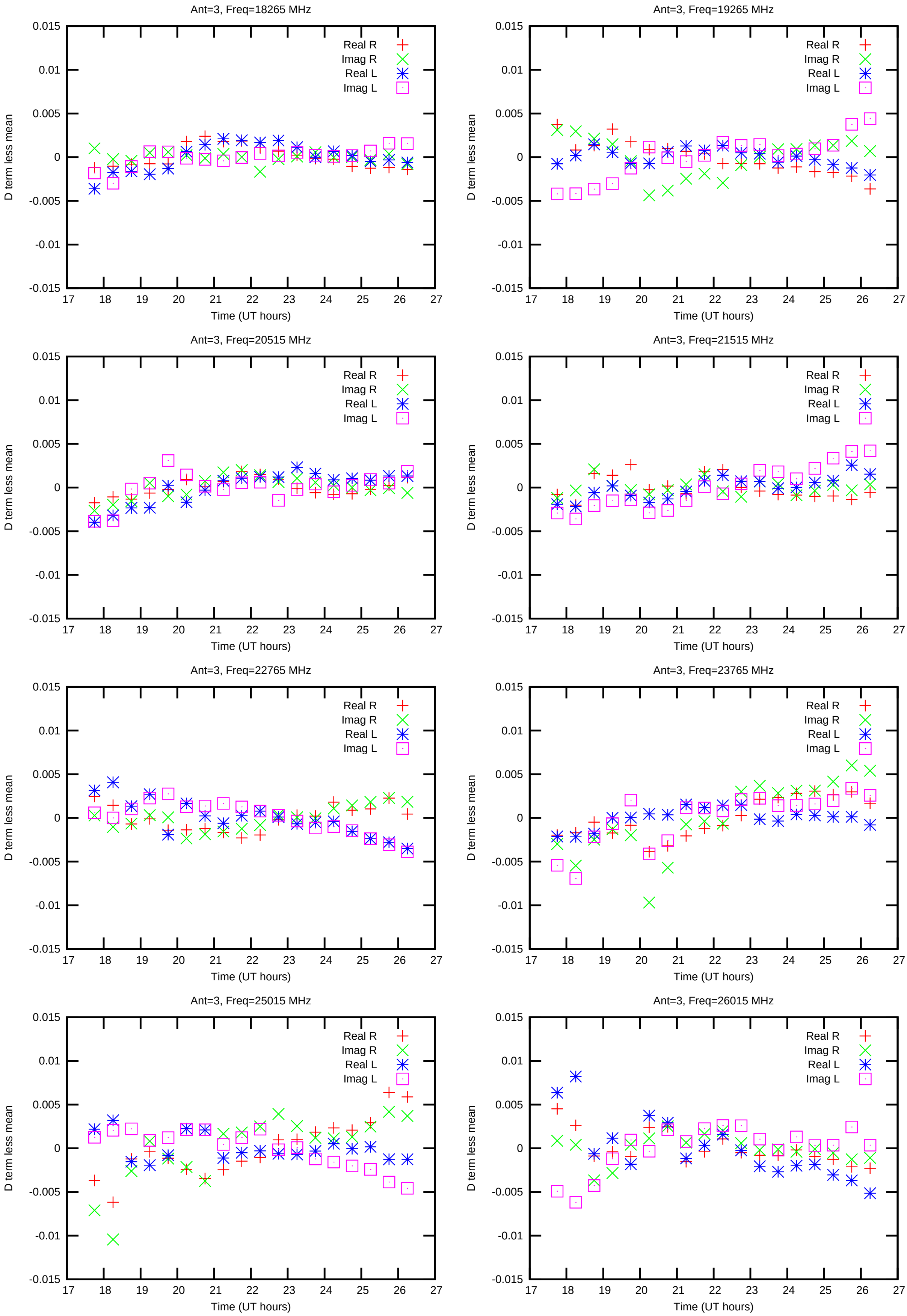

Figure 3: Polarization stability of antenna 3 at K-band. This is a typical well-behaved antenna.

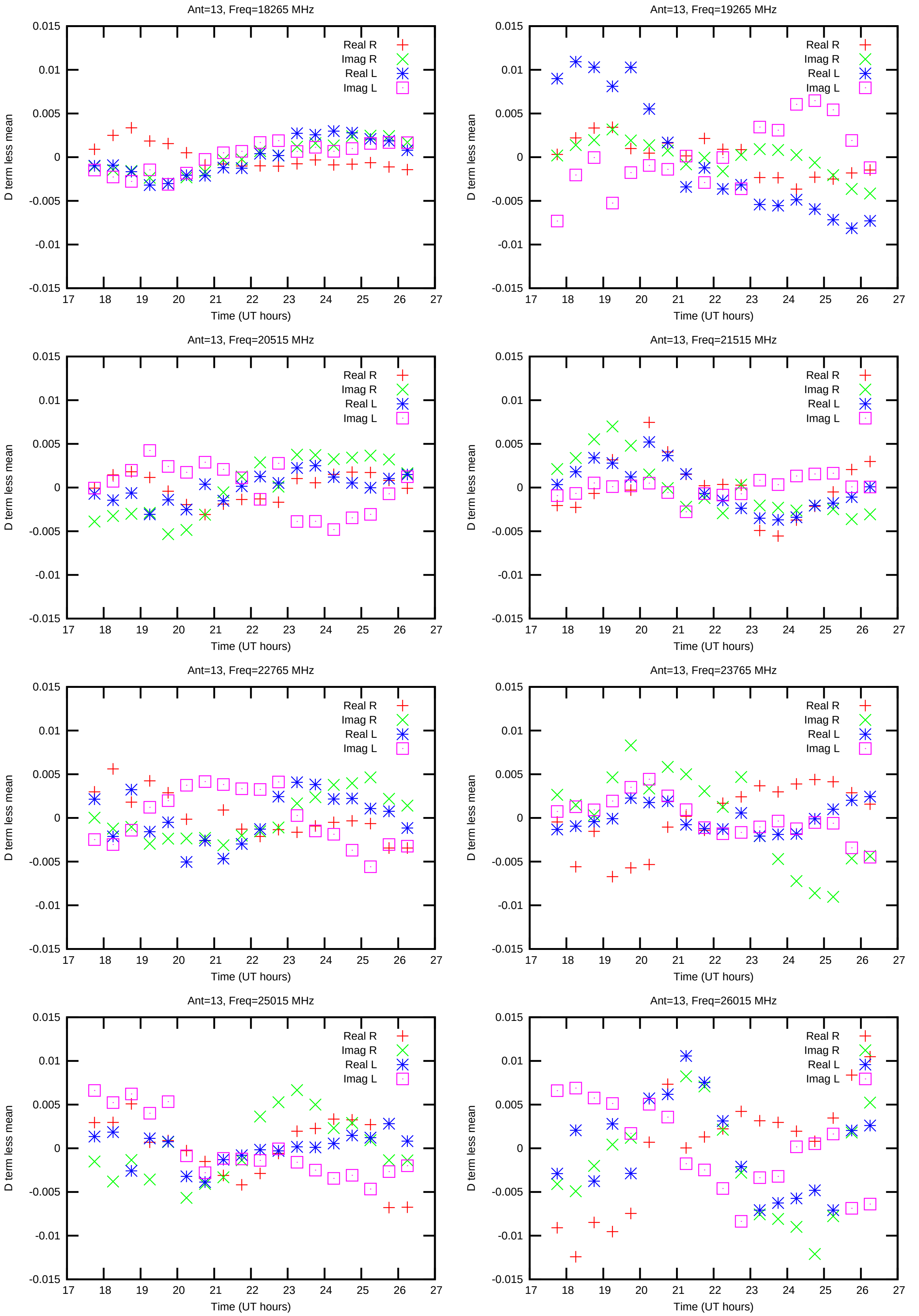

Figure 4: Polarization stability of antenna 13 at eight frequencies within K-band. This antenna is the most unstable of all.

To investigate the long-term stability, we took two observations at C-band, of two different sources (3C84 and 0217+738), separated by about two weeks. The results are shown in Figures 5 and 6. Both plots show the differences between the second day's polarization from the average value determined on the first day. As before the first figure shows a typical antenna. The change in cross-polarization is very small – typically 0.2%, and never more than 0.4%. The second figure shows that antenna 15 is unstable on long as well as short timescales, but even here, the median change over two weeks is typically only 0.5% – certainly small enough to enable good basic polarimetry without the need for polarization calibration.

8.4 Polarization Self-Calibration

Even with polarizer stability better than 10^{-3}, small fluctuations in the D-terms will scatter I-flux and limit polarimetric dynamic range in fields with very bright sources. In this case, the likely solution will be to employ the polarized emission itself to detect and remove the residual changes in polarization leakage – a form of self-calibration with direct analog to removing instrumental and atmospherically-induced phase fluctuations from Stokes 'I' images.

We have demonstrated this for the 25015 MHz data from 26 April. We assume the source polarization is stable and equal to the overall mean, and solve for the antenna-based leakage term on a half-hourly basis. The results are shown in Figure 7. The left panel shows how small residual variations of D scatter I flux throughout the image. Solving for and utilizing a time-variable D term enables noise-limited performance in Stokes Q as shown in the right hand panel However, the rms noise level in this images is still significantly above the theoretical noise limit. The thermal noise level is reached in observations of blank fields, while for calibrators such as 3C84, the noise levels are factors of a few above the noise. The discrepancy is under active investigation.

9 Conclusions

Polarizer stability over durations of a few hours in excellent at both C and K-bands, each representing one of the principal polarizer designs for the EVLA. The stability is sufficient to enable accuracy in on-axis fractional linear polarization of better than 0.1%. The stability of the K-band (waveguide design) polarizers appears to be about a factor of two worse than the OMT + quadrature hybrid polarizer design utilized at C-band. Despite this, the K-band polarization is certainly sufficiently stable for acccurate polarimetry.

Observations at C-band taken two weeks apart demonstrate that all antennas have excellent long-term polarization stability, certainly sufficient to ensure fraction linear polarization for on-axis observations of better than 1%.

For fields dominated by strong emission exceeding $\sim$ 1 Jy, it is likely that low-level polarizer variations will limit linear polarization sensitivity. For these cases, the strong source polarization can be used to monitor and remove polarizer variability. It is likely that for complex fields, a better procedure will be to utilize a nearby calibrator for such monitoring. Testing of the coherence in polarizer stability between two closely spaced calibrators will be conducted shortly, and reported elsewhere.

Further tests are underway to determine the long-term variability of the K, Ka, and Q-band polarizers. These results will be reported in an subsequent memo.

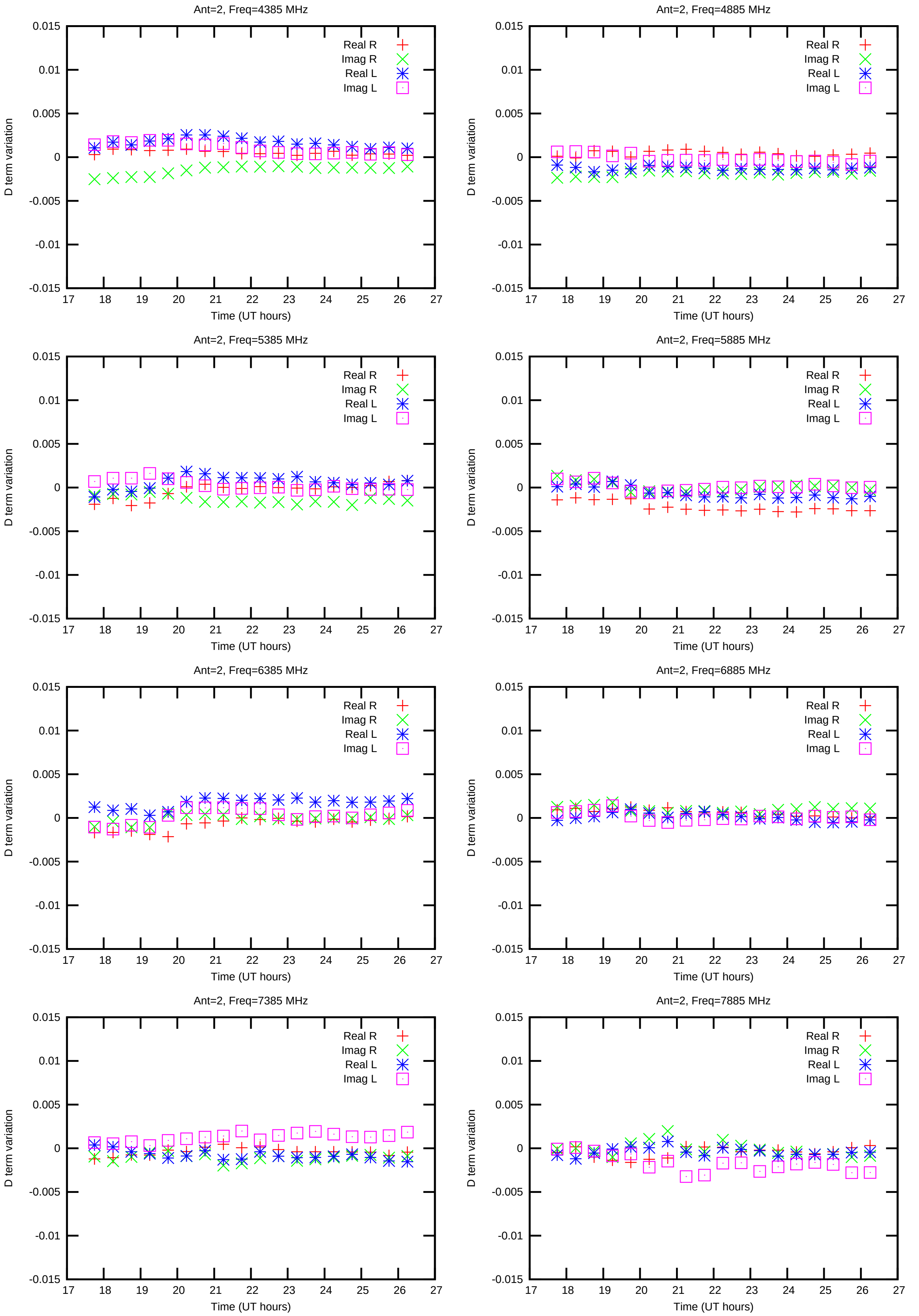

Figure 5: The change in the cross-polarization of antenna 2 at C-band over a two week period. The values shown are the differences between the value determined every half hour on April 26 from the mean value observed on April 12. This antenna is typical of the eight outfitted with wide-band polarizers.

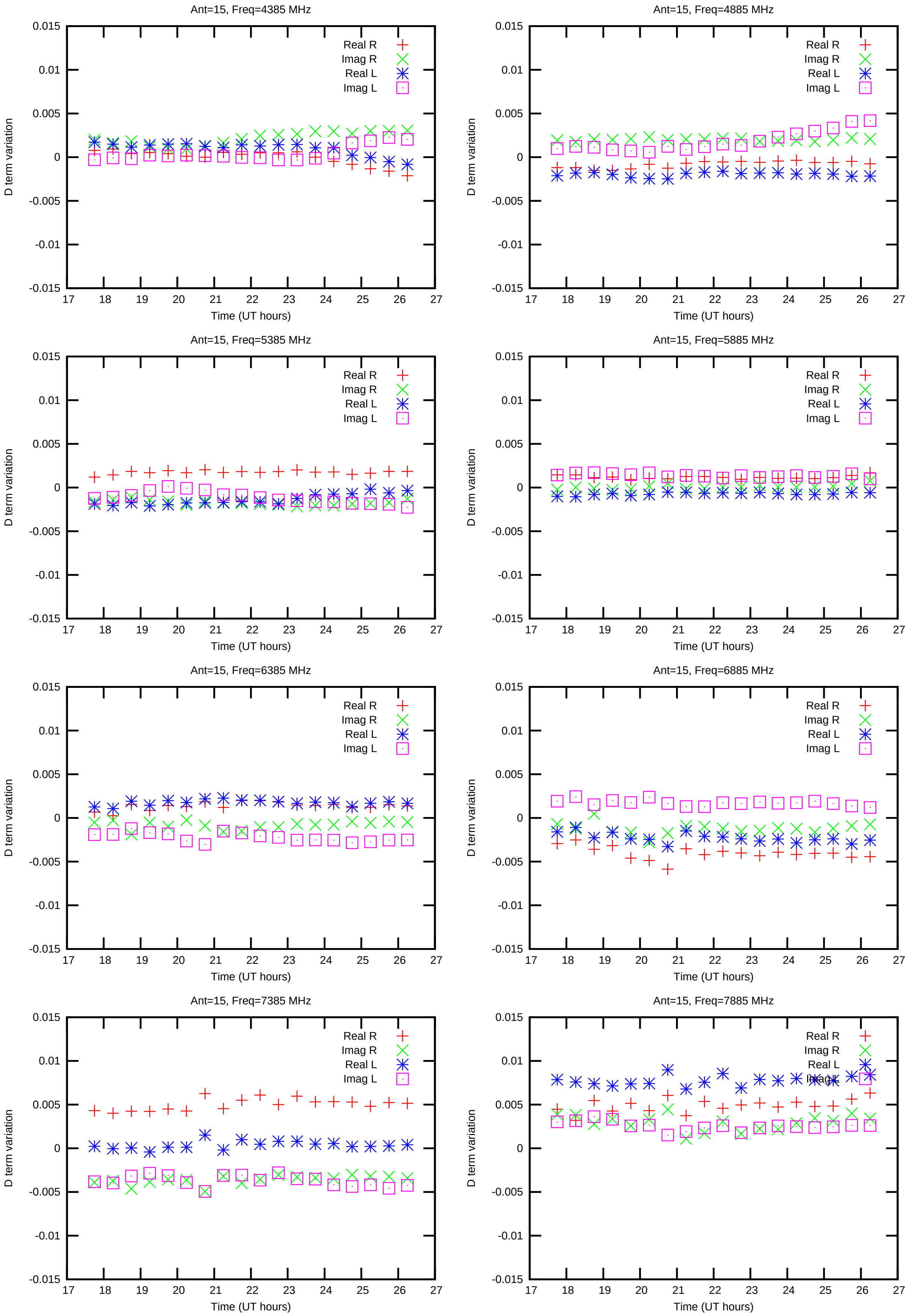

Figure 6: The change in cross-polarization of antenna 15 at C-band over a two-week period.

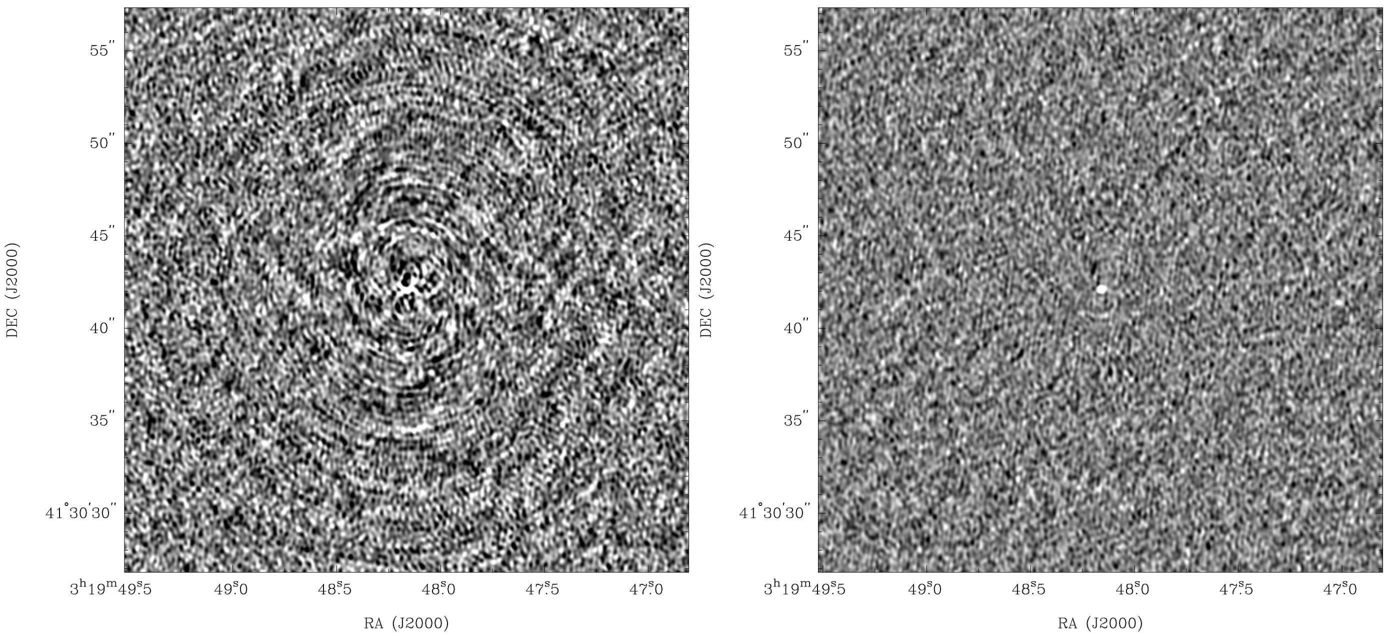

Figure 7: The left panel shows the Stokes Q image of 3C84 at K-band when a single polarization leakage solution is applied to all the data. Small variations in the D terms are scattering I flux, so that the noise in the image is well above the thermal level. The right panel shows the image after a time-variable D-term solution is enabled, where it is assumed the true source polarization is constant throughout the observation interval. Solutions were made and applied half-hourly. The scattered I-flux is removed to a level beneath the noise. The fractional polarization of 3C84 is 0.053% in this image, a factor of 20 above the rms noise.